ELSEVIER

Intermetallics 7 (1999) 179–184

Intermetallics

Phase stability, bonding mechanism, and elastic constants of Mo_5Si_3 by first-principles calculation

C.L. Fu [a,*], Xindong Wang [a], Y.Y. Ye [b], K.M. Ho [b]

[a] *Metals and Ceramics Division, Oak Ridge National Laboratory, PO Box 2008, Oak Ridge, TN 37831-6114, USA*
[b] *Ames Laboratory, US Department of Energy, Department of Physics and Astronomy, Iowa State University, Ames, IA 50011, USA*

Received 2 February 1998; accepted 26 March 1998

Abstract

We present results of first-principles local-density-functional calculations of the structural and elastic properties of Mo_5Si_3. Among the three different structures ($D8_m$, $D8_8$, and $D8_l$), the $D8_m$ structure (referred to as the T1 phase) has the greatest binding with a high heat of formation of −3.8 eV/formula unit. The bonding in Mo_5Si_3 is found to have pronounced covalent components, characterized by the planar Mo–Si–Mo triangular bonding units on the (001) plane and by the unusually short Mo–Mo bonds directly along the c-axis. The calculated six elastic constants of the $D8_m$ structure are in excellent agreement with the experimental values. While the bonding in the (001) basal plane is stronger than the bonding along the [001] direction (i.e. $C_{11}+C_{12}>C_{33}$ and $C_{66}>C_{44}$), the crystal anharmonicity is found to be higher along the [001] direction. The implication of our results on the anisotropy of thermal expansion coefficients is briefly discussed. © 1999 Elsevier Science Ltd. All rights reserved.

Keywords: Mo_5Si_3; First-principles calculation; Phase stability; Elastic constants; Thermal expansion coefficients

1. Introduction

Transition metal silicides constitute a unique class of intermetallic alloys for ultrahigh-temperature application [1]. Among the compounds of molybdenum silicides, $MoSi_2$ has been the most studied phase in the last several decades. Recently, due to advancements in the processing of materials, there is a growing interest in Mo_5Si_3 based alloys, because of their high strength and excellent creep resistance at high temperature (above 1400°C) [1–3]. Good oxidation resistance can also be achieved by additions of boron to Mo_5Si_3 [3,4]. Unfortunately, similar to most high-temperature intermetallics, these 5–3 silicides are too brittle at ambient temperature to be used as structural engineering materials. At present, only limited scientific effort has been focused on understanding (and improving) their brittle fracture behavior.

The 5–3 transition metal silicides have complex crystal structures. The binary Mo_5Si_3 is stabilized in a body-centered tetragonal structure of space group I4/mcm with the W_5Si_3-type structure ($D8_m$ structure, c.f. Fig. 1). A competing structure often observed in 5–3 silicides is the hexagonal structure. This hexagonal structure has a space group of $P6_3$/mcm with the Mn_5Si_3-type structure ($D8_8$ structure). With the addition of boron in Mo–Si, a ternary T2 (Mo_5SiB_2) phase is observed to form in the microstructures. The T2 phase has the I4/mcm space group with the Cr_5B_3-type structure (or $D8_l$ structure).

Recently, the lattice parameters, elastic constants and thermal expansion coefficients of Mo_5Si_3 have been measured by Chu et al. [5]. In collaboration with this effort, in this paper we report the results of first-principles calculations of the phase stability, bonding mechanism, and elastic properties of binary Mo_5Si_3 by the local-density-functional (LDF) approach. We find that the heat of formation is high, and the bonding is characterized by pronounced multi-centered covalent components in this alloy. We also briefly discuss the physical origin underlying the observed anisotropy in the thermal expansion coefficients along the [100] and [001] directions. In Section 2, a description on the theoretical methods is given. Results and discussion are given in Section 3.

* Corresponding author. Tel.: +1-423-574-5161; fax: +1-423-574-7659; e-mail: fucl@ornl.gov

0966-9795/99/$—see front matter © 1999 Elsevier Science Ltd. All rights reserved
PII: S0966-9795(98)00018-1

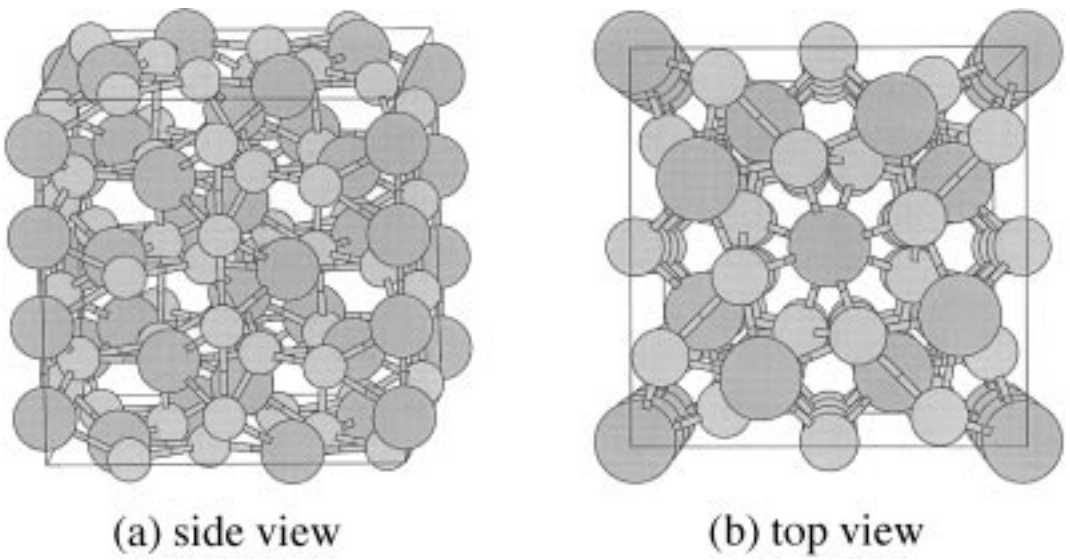

Fig. 1. The crystal structure of the W_5Si_3-type $D8_m$ structure. The larger darker atoms are Si atoms and the smaller lighter atoms are transition metal atoms.

2. Theoretical approach

We used the full-potential linearized augmented plane-wave (FLAPW) method [6] to solve the LDF equations. There is no shape approximation to the potential and charge density in this method. In this investigation angular momentum components up to $l=8$ and approximately 70 plane waves per atom were used for expansion of the wave functions. The semi-core 4p states of Mo are treated in two different ways: (1) as core states, and (2) as valence states but at a separate 'window' from the valence 4d, 5s and 5p states. We find these two models, however, give nearly identical results for the lattice parameters and elastic constants. The atomic positions are relaxed by calculating Hellmann–Feynman forces acting on the atoms.

A mixed-basis pseudopotential method [7] within the local density approximation was also used to investigate the phase stability. The pseudopotential method allows a more accurate treatment for the semi-core 4p states by directly incorporating them as the valence states. The use of two independent electronic band structure methods in this investigation also offers a measurement of the numerical precision of our calculations.

In order to determine the six elastic constants of the tetragonal $D8_m$ structure, a set of six independent total-energy calculations are performed. The lattice is deformed uniformly in six different ways, and for each of them we calculate the total energy as a function of strains (up to 2–3%). The new lattice axes a_i' are related to the original ones a_j by $a_i' = (1+\varepsilon_{ij})a_j$, where

$$\varepsilon_{ij} = \begin{bmatrix} e_1 & e_6/2 & e_5/2 \\ e_6/2 & e_2 & e_4/2 \\ e_5/2 & e_4/2 & e_3 \end{bmatrix}$$

is the strain tensor, and e_i are the strain components. The strain energy, U, is related to the elastic constants C_{ij} by

$$U = C_{ij}e_ie_j/2$$

The elastic constants C_{ij} are then obtained from the curvature of the total energy–strain curves.

3. Results and discussion

3.1. Phase stability

We start by considering two possible structures for binary Mo_5Si_3: $D8_m$ and $D8_8$ structures. The stacking sequence of layers along the c-axis can be viewed as repeated ABAC... stacking for both structures. The A-layer has a more open atomic environment (i.e. lower atomic packing density), which links together with the more close-packed B- and C-layers through the transition metal–silicon bonds. On the other hand, there is a direct coupling between A-layers, since the interatomic distance between atoms on adjacent A-layers is very short. The atomic arrangement of B-layer and C-layer are related by a 180° rotation about the c-axis for the $D8_8$ structure, and by reflections through planes containing the fourfold axis for the $D8_m$ structure. For both structures, we minimize the total energies with respect to both unit cell volume and c/a ratio. The heat of formation is then given by $E(Mo_5Si_3)-5E(Mo)-3E(Si)$ per formula unit, where $E(Mo_5Si_3)$, $E(Mo)$ and $E(Si)$ are the total energies of Mo_5Si_3, bulk Mo and bulk Si, respectively.

Calculations using both FLAPW and pseudopotential methods show that the ground state structure of

binary Mo_5Si_3 is, indeed, the W_5Si_3-type $D8_m$ structure (usually referred to as the T1 phase). The calculated heats of formation are nearly identical (to within 0.1 eV/formula unit) for both methods, indicating the precision of our calculations. The heat of formation for the $D8_m$ structure is high (−3.8 eV/formula unit), which suggests the existence of strong bonds in this compound. The difference in the heats of formation between the $D8_m$ and $D8_8$ structures is found to be considerable (i.e. about 0.7 eV/formula unit). It is thus not surprising that, in this case, the $D8_8$ structure can only be stabilized by interstitial alloying additions (for example, carbon; and is usually referred to as a Nowotny phase) [8], since the $D8_8$ structure is able to provide column-like holes to accommodate interstitial impurities.

The calculated lattice parameters of the $D8_m$ structure ($a = 9.59$ Å and $c = 4.85$ Å) are smaller than the experimental values, recently measured by Chu et al. [5], by about 1% (which is a common error inherent in the LDF calculation). It is worth mentioning that both $D8_m$ and $D8_8$ structures are characterized by a very narrow interlayer spacing along the c-axis. In the $D8_m$ structure, the shortest distance between Mo atoms on adjacent A layers along the c-axis is about 2.42 Å, in contrast to the first nearest neighbor distance of 2.72 Å in bulk bcc-Mo. On the other hand, the Si–Mo distances are nearly constant (i.e. about 2.55 Å), indicating that the Si–Mo bonding is dominant. For the $D8_8$ structure, the calculated lattice parameters are $a = 7.29$ Å and $c = 5.0$ Å, which corresponds to a Mo–Mo distance of 2.5 Å along the c-axis. (Similarly, we have examined Ti_5Si_3 stabilized in the $D8_8$ structure. In this case, the shortest distance between Ti atoms is about 2.54 Å, which is much shorter than the Ti–Ti distance of 2.89 Å in bulk hcp-Ti.)

Our calculation gives the following atomic positions (in Cartesian coordinates) for Mo and Si in the unit cell of the $D8_m$ structure: two Si at (0,0,1/4) and (1/2,1/2,1/4), two Mo atoms at (0,1/2,1/4) and (1/2,1/2,1/4), four Si atoms at $\pm(x,1/2+x,0)$ and $\pm(1/2+x,-x,0)$ with $x = 0.168$, and eight Mo atoms at $\pm(x,y,0)$, $\pm(-y,x,0)$, $\pm(x,-y,1/2)$, and $\pm(y,x,1/2)$ with $x = 0.076$ and $y = 0.226$. The calculated atomic positions are in good agreement with those from X-ray diffraction measurements [9].

The pseudopotential method was used to calculate the heat of formation for the $D8_l$ structure of binary Mo_5Si_3. Lattice parameters of $a = 6.39$ Å and $c = 11.22$ Å are obtained, and a heat of formation of 2.6 eV. It shows that, in the absence of boron additions, the $D8_l$ structure of Mo_5Si_3 has a higher energy than both the $D8_m$ and $D8_8$ structures.

To investigate the electronic structure underlying the calculated structural stability, in Fig. 2 we show the calculated electron density-of-states (DOS) for both the $D8_m$ and $D8_8$ structures. The Mo–Si bonding states are fully occupied with the center of the band located at about 4 eV below the Fermi level. The states near the Fermi level are dominated by Mo d-states. While these two DOS profiles bear a lot of resemblance, a major difference exists in the location of the Fermi level. The Fermi level in the $D8_m$ structure is located at a local minimum in the electron density-of-states. It is generally believe that a reduction in DOS at the Fermi level contributes to the stability of a given structure. This can be easily understood in the case of covalently-bonded materials where a Fermi level gap in the DOS is obviously a stabilizing effect. It corresponds to the situation where all bonding electronic states are occupied and all the non-bonding states are empty. In the intermetallic compounds discussed here, even though a full gap does not exit, the reduction in DOS at the Fermi level is still believed to have some stabilizing effect. From Fig. 2, we can clearly see that the Fermi level of the $D8_8$ structure is located away from the local minimum in the DOS profile, and this explains the large energy difference between the $D8_m$ and $D8_8$ structures.

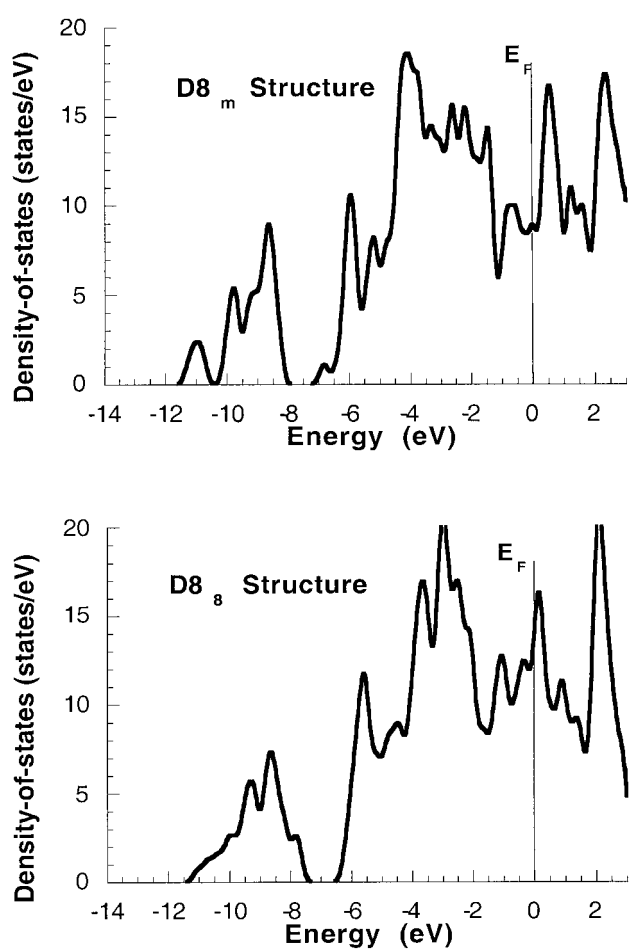

Fig. 2. Electron density-of-states for Mo_5Si_3 in $D8_m$ and $D8_8$ structures. E_F is the position of Fermi level.

3.2. Bonding charge density

To understand the bonding behavior involving the microscopic charge transfer and the formation of directional bonds (which is one of the characteristics of silicides), we have examined the bonding (or deformation) charge density. The bonding charge density is the difference between the charge density in the crystal and the superposition of neutral Mo and Si atomic charge densities at the lattice sites. This is the electronic density which can be measured experimentally by electron diffraction microscopy.

Following the notations introduced in the last section for the layer stacking along the c-axis, we present in Fig. 3 the bonding charge density for the $D8_m$ structure on (a) the B- or C-layer (i.e. (001) plane) and (b) the (100) plane intersecting Mo and Si atoms on the A-layers.

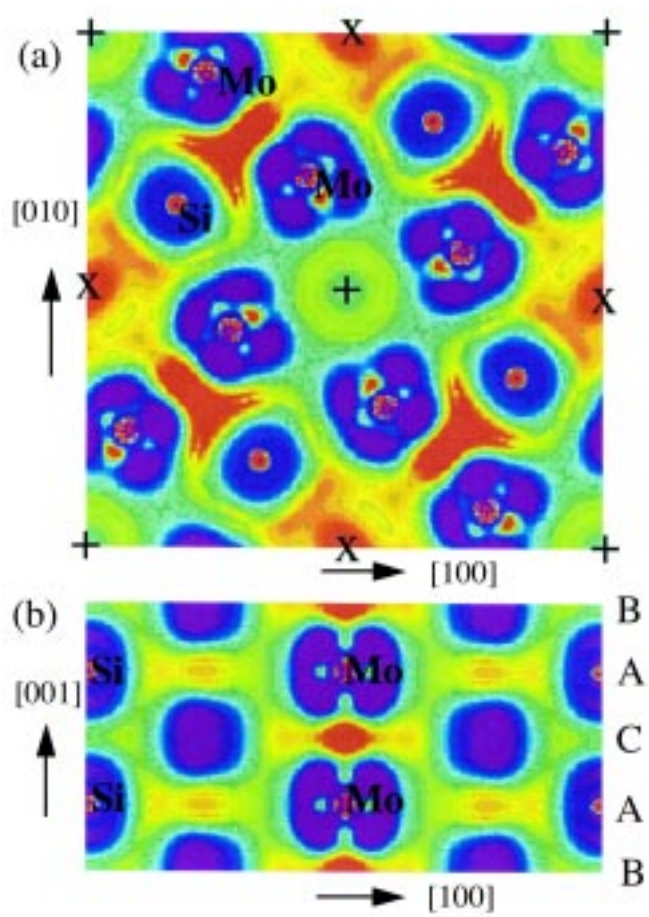

Fig. 3. Bonding charge density on (a) the (001) plane, and (b) the (100) plane of Mo_5Si_3 with the $D8_m$ structure. Symbols × and + in (a) denote the positions of out-of-plane Mo and Si atoms, respectively. The vertical direction in (b) is the c-axis. The red (purple) colors denote regions of increased (decreased) electronic density as the atoms are brought together to form a crystal (see text for details). The increase of electronic density in (a) is centered in the interstitial region shared among Mo–Si–Mo atoms (i.e. multi-centered covalent bonding). There also exists a covalent bonding between Mo atoms on adjacent A-layers.

These plots show the depletion of electronic density at the lattice sites (denoted by purple color) together with a significant increase of electronic density in the interstitial region (denoted by red and yellow colors). In Fig. 3, the regions where the increased electronic density is larger than 1.0×10^{-2} electrons/(a.u.)^3 are emphasized by red color. The maximum of the increased density in the interstitial region is considerable, which has a value about 1.8×10^{-2} electrons/(a.u.)^3.

The bonding characteristic on the more close-packed (001) plane is found to be dominantly covalent [c.f. Fig. 3(a)]. There is a pronounced planar triangular bonding among Mo–Si–Mo atoms. These planar triangular bonding units are then linked together in the ⟨110⟩ directions through the bonding of in-plane Si atoms and out-of-plane Mo atoms [with the projected positions marked by × symbols in Fig. 3(a)].

We have also examined the bonding characteristics of interlayer coupling along the c-axis [c.f. Fig. 3(b)]. We do not find noticeable directional bonds between Si atoms on adjacent A-layers, and between Si atoms on the A-layer with Mo atoms on the B-layer (or C-layer). On the other hand, the covalent bonding between Mo atoms on adjacent A-layers along the c-axis is obvious. These Mo atoms are coupled together with Si atoms on the B-layer (and C-layer) to form a muti-centered bond. This multi-center covalent bond is characterized by a very short Mo–Mo bond length.

Thus, the built-up electronic densities in Mo_5Si_3 with the $D8_m$ structure are mostly planar and localized on the more close-packed (001) plane (i.e. B- and C-layers). These multi-centered bonds, however, involve both in-plane and out-of-plane bonding components. The in-plane bonding is dominated by the planar Mo–Si–Mo triangular bond. On the other hand, the interlayer coupling has a covalent Mo–Mo bonding component with unusually short bond length.

3.3. Elastic properties

To determine six elastic constants, we need six relations, which can be obtained by considering the following strain tensors: (i) $e_1=e_2=e$ and $e_3=(1+e)^{-2}-1$, that is, tetragonal distortion at a fixed volume; (ii) $e_1=e_2=e$; (iii) $e_3=e$; (iv) $e_6=e$; (v) $e_4=e_5=e$; and (vi) $e_1=-e_2=e$, where the unspecified strain components are zero for each of these cases. Therefore, six relations (i) $U=(C_{11}+C_{12}+2C_{33}-4C_{13})e^2$, (ii) $U=(C_{11}+C_{12})e^2$, (iii) $U=1/2C_{33}e^2$, (iv) $U=1/2C_{66}e^2$, (v) $U=C_{44}e^2$, and (vi) $U=(C_{11}-C_{12})e^2$ are obtained for the distortion energies. We calculated the total energies according to the above six kinds of lattice distortions and fitted the calculated values to third-order polynomials to get the elastic constants.

At the theoretical lattice parameters of the $D8_m$ structure, we obtain $C_{11}=487$ GPa, $C_{12}=175$ GPa,

$C_{33}=420$ GPa, $C_{13}=145$ GPa, $C_{44}=120$ GPa, and $C_{66}=160$ GPa. Other than C_{12} and C_{13}, the calculated elastic constants at the theoretical volume are larger than the experimental values, measured by Chu et al. [5] by about 10%. This discrepancy is mostly due to the error in the calculated lattice constant. That is, in addition to having a higher energy density, the effect of crystal anharmonicity also gives rise to larger elastic constants at a smaller volume. We have subsequently calculated the elastic constants at the measured lattice constants. Indeed, we find excellent agreement between theory and experiment if the calculations are done at the measured lattice constants. The calculated elastic constants together with the measured values are summarized in Table 1.

The calculated (and measured) elastic constants are consistent with the fact that the bonding in the (001) plane is stronger than the bonding along the [001] direction. This is evident with the following relations: $C_{11}+C_{12}>C_{33}$ and $C_{66}>C_{44}$. The former indicates that the elastic tensile modulus is higher on the (001) plane than along the c-axis. The latter suggests that the [100](001) shear is easier than the [100](010) shear (i.e. for the (001) layers, the shear of interlayer bonds is easier than the shear of intralayer bonds). It is also interesting to note that the shear anisotropy ratio A, defined as

$$A = 2C_{66}/(C_{11} - C_{12})$$

is nearly equal to one ($A=0.98$), indicating that the shear elastic properties of the (001) plane are nearly independent of shear directions.

An important experimental observation relating to the elastic properties is the anisotropy in the thermal expansion along the [001] and [100] directions [5]. The thermal expansion coefficient in the [001] direction is observed to be more than twice of that in the [100] direction. We have calculated the thermal expansion coefficients. The calculated results for Mo_5Si_3 together with other Mo–Si alloys will be published elsewhere. Here we will only briefly describe the physical origin for the observed anisotropy in terms of the calculated electronic structure.

Table 1
Elastic constants (GPa) of Mo_5Si_3. The two sets of theoretical values are calculated at the theoretical and experimental unit cell volumes, respectively

	C_{11}	C_{12}	C_{33}	C_{13}	C_{44}	C_{66}
Theory (theoretical volume)	487	175	420	145	120	160
Theory (experimental volume)	438	162	371	132	106	143
Experiment[a]	446	174	390	140	110	140

[a] Ref. [5].

The thermal expansion coefficient depends not only on the second-order elastic constants but also on crystal anharmonicity. In the present case, since $C_{11}+C_{12}$ is larger than C_{33}, the bonding in the (001) plane is more elastically rigid than along the c-axis. On the other hand, we can describe the anharmonic effects in the vibrating lattice in terms of a Grüneisen constant, γ, defined as

$$\gamma = -\frac{\partial \ln \theta_D}{\partial \ln V}$$

which gives the volume dependence of the Debye temperature, θ_D. We find that the anharmonicity is higher in the [001] direction ($\gamma_{[001]} = 2.55$) than in the [100] direction ($\gamma_{[100]} = 2.17$). A stronger bonding in the (001) plane together with a higher anharmonicity along the [001] direction contribute to a higher thermal expansion coefficient along the [001] direction than along the [100] direction.

A major contribution to the anisotropy in anharmonicity comes from the difference in the anharmonicity of C_{44} along the [001] and [100] directions. We find that the anharmonicity of C_{44} is higher along the [001] direction. It should be noted that, in the present case, the C_{44} shear does not significantly affect the Mo–Si–Mo planar bonding on the (001) plane. The C_{44} value predominantly manifests the elastic shear strength of interlayer coupling. As mentioned already, the structure of Mo_5Si_3 is characterized by a narrow (001) interlayer spacing with a very short Mo–Mo bond directly along the c-axis. This short Mo–Mo bond is coupled with the Si atoms on the B- and C-layers to form a multi-centered covalent bond. The anharmonicity of C_{44} is calculated to be higher with respect to the lattice expansion along the [001] direction than along the [100] direction, because an increase of the [001] lattice spacing is more effective in reducing the bonding strength of this Mo–Mo covalent bond and making the C_{44} shear easier.

4. Summary

We have presented results of first-principles calculations for the phase stability, bonding mechanism and elastic properties of Mo_5Si_3. The bonding in Mo_5Si_3 is dominated by the multi-centered covalent bonding components. While the planar Mo–Si–Mo bonding on the (001) plane is dominant, covalent bonding between Mo atoms at adjacent A-layers is important in interlayer coupling. The heat of formation for the $D8_m$ structure is high (−3.8 eV/formula unit), which is 0.7 eV lower than that of the competing $D8_8$ structure. The stabilization of the $D8_m$ structure (T1 phase) is due to the reduction in electron density-of-states at the Fermi level. The calculated elastic constants for the $D8_m$

structure are in good agreement with experimental measurement. Consistent with a stronger bonding in the (001) plane than along the c-axis, we have the relations: $C_{11}+C_{12}>C_{33}$ and $C_{66}>C_{44}$. The crystal anharmonicity is found to be larger along the [001] direction than along the [100] direction, largely because the softening of the shear C_{44} term with respect to lattice expansion is more pronounced along the [001] direction.

Acknowledgements

Research at ORNL was sponsored by the Division of Materials Sciences, Office of Basic Energy Sciences, US Department of Energy under contract DE-AC05-96OR22464 with Lockheed Martin Energy research Corporation. Ames Laboratory is operated for the US Department of Energy by Iowa State University under Contract No. W-7405-Eng-82.

References

[1] Shah DM, Berczik D, Anton DL, Hecht R. Mat Sci Eng 1992;A155:45.
[2] Anton DL, Shah DM. Mat Res Soc Symp Proc 1991;213:733.
[3] Meyer MK, Kramer MJ, Akinc M. Intermetallics 1996;4:273.
[4] Meyer MK, Akinc M. J Am Ceram Soc 1996;79:938.
[5] Chu F. et al. Intermetallics, submitted.
[6] Wimmer E, Krakauer K, Weinert M, Freeman AJ. Phys Rev 1981;B24:864.
[7] Louie SG, Ho KM, Cohen ML. Phys Rev 1979;B19:1774.
[8] Nowotny H, Parthe E, Kieffer R, Benesovsky F. Monatsh Chem 1954;85:255.
[9] Naidu SVN, Mays CF, Houska CR. Comm Am Ceram Soc 1982;65:58.